Age of Information in Slotted ALOHA With Energy Harvesting

Khac-Hoang Ngo*, Giuseppe Durisi*, Alexandre Graell i Amat*, Andrea Munari†, and Francisco Lázaro†
*Department of Electrical Engineering, Chalmers University of Technology, 41296 Gothenburg, Sweden
†Institute for Commonications and Navigation, German Aerospace Center (DLR), 82234 Weßling, Germany

***Abstract*—We examine the age of information (AoI) in a status update system that incorporates energy harvesting and the slotted ALOHA protocol. We derive analytically the average AoI and the probability that the AoI exceeds a given threshold. Via numerical results, we investigate the trade-off between i) transmitting a new update whenever possible, and ii) transmitting only when sufficient energy is available to increase the chance of successful delivery. The two strategies turn out to be beneficial for low and high update generation rates, respectively. However, an optimized approach that balances the two strategies outperforms them significantly in terms of both AoI and throughput.**

I. Introduction

In delay-sensitive Internet of Things (IoT) applications, devices need to deliver timely status updates to a central gateway. To measure the freshness of status updates, the age of information (AoI) metric has been introduced (see, e.g., [1] and references therein). It captures the time elapsed since the generation of the last update available at the gateway. Recent studies have characterized the AoI for random-access medium sharing protocols, such as slotted ALOHA [2], [3] and its more advanced variations [4], [5].

IoT devices are designed for low-power, long-term operation and can be placed in remote or hard-to-reach locations, hindering battery replacement. A solution to these challenges is energy harvesting, which allows IoT devices to capture and convert energy from the environment into electrical energy [6]. Existing analyses of ALOHA-based random-access protocols with energy harvesting focused on stability [7] and throughput [8], [9]. Compared to the setting in [2]–[5], energy harvesting introduces new factors that significantly affect information freshness, such as the level of available energy at the devices at the time of update generation, and the need for the devices to spend time harvesting energy. However, the impact of energy harvesting on the AoI in random-access protocols remains widely unexplored.

This paper characterizes the behavior of the AoI metric in a slotted ALOHA system with energy harvesting. We model energy arrivals as independent Bernoulli processes. We assume that each device receives readings from a sensor, and thus cannot generate fresh updates at will. Upon having an update, the device transmits the update with a probability adapted to its battery level. Assuming that each slot comprises multiple uses of an additive white Gaussian noise (AWGN) channel, we evaluate the successful delivery probability of an update, given the battery level of its transmitter and the battery profile of the other devices. We also consider decoding with capture, where the receiver attempts to decode every packet transmitted in a slot using successive interference cancellation (SIC). By means of a Markovian analysis, we derive the average AoI analytically for a given battery-dependent transmission probability. We further provide an approximate analysis that results in easy-to-compute and accurate approximations of both average AoI and age-violation probability (AVP), i.e., the probability that the AoI exceeds a given threshold.

We then investigate the importance of optimally adapting the transmission probability to the available energy. On the one hand, transmitting a new update whenever possible exploits every opportunity to reduce the AoI, but increases channel traffic and the risk of losing the update if the transmit power is insufficient. On the other hand, transmitting only with high power increases the chance of successful delivery, but requires devices to ignore some updates while harvesting enough energy. Taking these two cases as baselines, we compare them with the optimized transmission probability that minimizes the average AoI, minimizes the AVP, or maximizes the throughput. Numerical results show that significant gains in all three metrics are achieved with the optimized strategy. For low update generation rates, transmitting a new update whenever possible is close to optimal. However, for high update generation rates, this strategy performs poorly, while transmitting only when sufficient energy is available is close to optimal in the case without capture. Furthermore, we show that the transmission probability optimized for the AoI also performs well in terms of throughput, and vice versa. Finally, decoding with capture outperforms significantly decoding without capture.

We denote $[m:n] = \{m, m+1, \dots, n\}$, $[n] = [1:n]$, and $x^+ = \max\{0, x\}$. We denote by $\mathbf{I}_m$, $\mathbf{0}_m$, and $\mathbf{1}_m$ the $m \times m$ identity matrix, $m \times 1$ all-zero vector, and $m \times 1$ all-one vector, respectively. The first entry of vector $\boldsymbol{x}$ is denoted by $[\boldsymbol{x}]_1$.

II. System Model

We consider a system with U devices attempting to deliver time-stamped status updates (also referred to as packets) to a receiver through a wireless channel. Time is slotted and the devices are slot-synchronous. Each update transmission spans a slot. A device has a new update at the beginning of each slot with probability (w.p.) α independently of the other devices.

This project has received funding from the European Union's Horizon 2020 research and innovation programme under the Marie Skłodowska-Curie grant agreement No 101022113, and from the Swedish Research Council under grant 2021-04970.

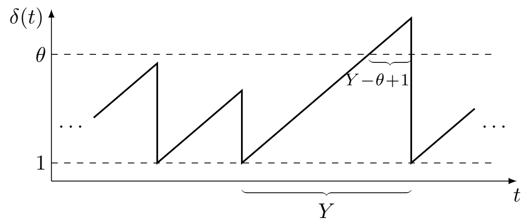

Fig. 1: Example of the AoI process.

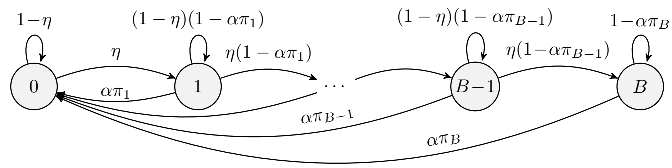

Fig. 2: Markov chain $\mathcal{M}_1$ describing the battery level of a device.

1) Energy Harvesting: Each device is equipped with a rechargeable battery with capacity B energy units. The devices harvest energy from the environment to recharge their batteries. In each slot, one energy unit is harvested by a device w.p. η, independently of the other slots and other devices. If the battery is full, the device pauses harvesting. We denote by ν_b (computed in Section III) the steady-state probability that the battery level of an arbitrary device is $b \in [0 : B]$.

2) Medium Access Protocol: The devices access the medium following the slotted ALOHA protocol. Specifically, if a device has a new update in a slot, it transmits the update w.p. π_b if its battery level is b. An old update is never sent. Obviously, $\pi_0 = 0$, while $\boldsymbol{\pi} = [\pi_1 \dots \pi_B]$ is a design parameter. A packet is always transmitted with all available energy. Furthermore, as in [7], [8], we assume that the devices can either transmit or harvest energy in a slot. No feedback is provided by the receiver.

Consider a device that transmits with b energy units in a slot where the *battery profile* of the remaining devices is $\boldsymbol{L} = [L_0 \ L_1 \dots L_B]$, i.e., L_i out of the remaining $U - 1$ devices have battery level $i \in [B]$. We denote by $w_{b,\boldsymbol{L}}$ the probability that the device of interest successfully delivers an update, given that it transmits. Note that $w_{b,\boldsymbol{L}}$ depends on the physical-layer channel model, which we shall present in Section III. At steady state, the average successful delivery probability of a device that transmits with b energy units is

$$\bar{w}_b = \mathbb{E}_{\boldsymbol{L}}[w_{b,\boldsymbol{L}}] \tag{1}$$

where $\boldsymbol{L}$ follows the multinomial distribution with number of trials $U - 1$, number of events $B + 1$, and event probabilities $\{\nu_i\}_{i=0}^B$, denoted by $\mathrm{Mult}(U-1, B+1, \{\nu_i\}_{i=0}^B)$. The average throughput, i.e., the average number of packets decoded per slot, is given by $S = \alpha U \sum_{b=0}^B \nu_b \pi_b \bar{w}_b$.

3) Age of Information: We define the AoI of a generic device at slot t as $\delta(t) = t - \tau(t)$, where $\tau(t)$ denotes the timestamp of the last received update from this device as of slot t. The corresponding stochastic process is denoted as $\Delta(t)$. The AoI grows linearly with time and is reset to 1 when a new update is successfully decoded. It has a saw-tooth shape as illustrated in Fig. 1. We are interested in the average AoI $\bar{\Delta} = \mathbb{E}[\Delta(t)]$ and the AVP $\zeta(\theta) = \mathbb{P}[\Delta(t) > \theta]$.

III. Battery Level and Successful Delivery Probability

A. Battery Level Evolution

1) Battery Level of a Generic Device: The evolution of the battery level of a generic device is captured by the Markov chain $\mathcal{M}_1$ shown in Fig. 2. Each state represents a battery level. The transition probabilities between the states can be readily computed. Specifically, a device in state 0 cannot transmit, thus it either remains in this state if it does not harvest energy (w.p. $1 - \eta$) or jumps to state 1 if an energy unit arrives (w.p. η). A device in state $i \in [B]$ moves to state 0 if it generates and transmits a new update (w.p. $\alpha\pi_i$). Otherwise, if $i < B$, the device either remains in state i if no energy is harvested (w.p. $(1 - \eta)(1 - \alpha\pi_i)$) or jumps to state $i + 1$ if an energy unit arrives (w.p. $\eta(1 - \alpha\pi_i)$). If the battery is full, i.e., $i = B$, the device remains in state B if it does not transmit (w.p. $1 - \alpha\pi_i$). From these transition probabilities, we compute the steady-state distribution $\{\nu_b\}_{b=0}^B$ by solving the balance equations.

2) Battery Profile of $U - 1$ Devices: The battery profile $\boldsymbol{L}$ of $U-1$ devices can take value in $\mathcal{L} = \big\{[\ell_0 \ \ell_1 \dots \ell_B] \colon \sum_{i=0}^B \ell_i = U-1, \ell_i \in [0 : U-1], i \in [0 : B]\big\}$. We now describe the evolution of $\boldsymbol{L}$ within a slot. Let $\boldsymbol{\ell}' = [\ell_0' \ \ell_1' \dots \ell_B']$ and $\boldsymbol{\ell} = [\ell_0 \ \ell_1 \dots \ell_B]$ denote the states at the beginning and the end of a slot, respectively. Let also $u_{j,k}$ be the number of devices whose battery goes from level j to k. We have that

$$u_{j,k} \in [0 : \min\{\ell_j', \ell_k\}], \quad j, k \in [0 : B], \tag{2}$$
$$\ell_0' = u_{0,0} + u_{0,1}, \tag{3}$$
$$\ell_i' = u_{i,i} + u_{i,0} + u_{i,i+1}, \quad i \in [1 : B-1], \tag{4}$$
$$\ell_B' = u_{B,B} + u_{B,0}, \tag{5}$$
$$\ell_0 = u_{0,0} + \textstyle\sum_{i=1}^B u_{i,0}, \tag{6}$$
$$\ell_i = u_{i,i} + u_{i-1,i}, \quad i \in [B]. \tag{7}$$

The transition probabilities between profiles of $U-1$ devices is

$$\mathbb{P}[\boldsymbol{\ell}' \to \boldsymbol{\ell}] = \sum_{\{u_{j,k}\}:\,(2)\text{–}(7)} \Bigg(\prod_{j,k\in[0:B]} p_{j,k}^{u_{j,k}} \Bigg) \cdot \binom{\ell_0'}{u_{0,0}} \binom{\ell_B'}{u_{B,0}} \prod_{j=1}^{B-1} \binom{\ell_j'}{u_{j,0}} \binom{\ell_j' - u_{j,0}}{u_{j,j}}, \tag{8}$$

where $p_{j,k}$ is the transition probability from state j to state k of the Markov chain $\mathcal{M}_1$ in Fig. 2.

B. Successful Delivery Probability

We assume that a slot comprises n uses of a real-valued AWGN channel. In a slot, active device i with battery level b_i transmits a signal $\boldsymbol{x}_i \in \mathbb{R}^n$ ($\|\boldsymbol{x}_i\| = 1$) with power b_i/n. The received signal is $\boldsymbol{y} = \sum_{i=1}^K \sqrt{b_i/n}\, \boldsymbol{x}_i + \boldsymbol{z}$, where K is the number of active devices and $\boldsymbol{z} \sim \mathcal{N}(0, \sigma^2)$ is the AWGN. The devices transmit at rate R bits/channel use, i.e., $\boldsymbol{x}_i$ belongs to a codebook containing 2^{nR} codewords. We consider shell codes for which the codewords are uniformly distributed on the unit sphere. We consider two decoding scenarios.

1) Without capture: In this scenario, all collided packets are lost. Decoding is attempted only on packets transmitted in singleton slots. This model allows us to revisit the collision channel model commonly used in modern random-access analyses, and further account for single-user decoding errors due to finite-blocklength effects. Consider an active device that transmits with b energy units while the battery profile of the remaining $U-1$ devices is $\boldsymbol{L}=[L_0 \dots L_B]$. The successful delivery probability of the device of interest is

$$w_{b,\boldsymbol{L}} = (1-\epsilon_b)\prod_{i=0}^{B}(1-\pi_i)^{L_i}, \tag{9}$$

where ϵ_b is the error probability of decoding the device of interest in a singleton slot. To compute ϵ_b, we use that the maximum achievable rate is [10, Th. 54]

$$R^* = C(b) - \sqrt{\frac{V(b)}{n}}Q^{-1}(\epsilon_b) + O\big(\tfrac{\ln n}{n}\big) \tag{10}$$

where $C(b)=\frac{1}{2}\log_2\big(1+\frac{b}{n\sigma^2}\big)$, $Q^{-1}(\cdot)$ is the inverse of the Gaussian Q-function $Q(z)=\frac{1}{2\pi}\int_z^\infty e^{-t^2/2}\mathrm{d}t$, and $V(b)$ is the channel dispersion. Here, it follows from [11, Th. 1] that $V(b)=\frac{\frac{b^2}{n^2\sigma^4}+2\frac{b}{n\sigma^2}}{2(\frac{b}{n\sigma^2}+1)^2}\log_2^2(e)$. For a fixed rate R, we use (10) to approximate ϵ_b as $\epsilon_b \approx Q\Big(\sqrt{\frac{n}{V(b)}}(C(b)-R)\Big)$, where we omitted the term $O(\frac{\ln n}{n})$, which is negligible for large n.

2) With capture: In this case, the receiver attempts to decode every packet transmitted in a slot by treating all other colliding packets as noise. Consider an active device with battery level b and let the battery profile of the remaining $U-1$ devices be $\boldsymbol{L}=[L_0\dots L_B]$. Furthermore, assume that out of the other L_i devices with battery level i, $\bar{L}_i$ devices transmit. Then the interference-to-noise power ratio is $\tilde{P}=\frac{1}{n\sigma^2}\sum_{i=0}^{B} i\bar{L}_i$, and the signal-to-interference-plus-noise ratio is $\bar{P}=\frac{b/(n\sigma^2)}{\tilde{P}+1}$. In this setup, the maximum achievable rate for the device of interest is given as in (10) with $C(b)$ and $V(b)$ replaced by $\frac{1}{2}\log_2(1+\bar{P})$ and $V'(b,\{\bar{L}_i\})=\frac{\frac{b^2}{n^2\sigma^4}(1+2\tilde{P}+\tilde{P}^2-\check{P})+2\frac{b}{n\sigma^2}(\tilde{P}+1)^3}{2(\tilde{P}+1)^2(b/(n\sigma^2)+\tilde{P}+1)^2}\log_2^2 e$, respectively [11, Th. 2]. Here, $\check{P}=\frac{1}{n^2\sigma^4}\sum_{i=0}^{B} i^2\bar{L}_i$. Given $\{\bar{L}_i\}_{i=0}^{B}$, the error probability of the device is approximated as

$$\epsilon_{b,\{\bar{L}_i\}} \approx Q\Big(\sqrt{\tfrac{n}{V'(b,\{\bar{L}_i\})}}\big(\tfrac{1}{2}\log_2(1+\bar{P})-R\big)\Big). \tag{11}$$

We further assume that the receiver employs SIC. It first decodes all devices that transmit with B energy units, removes the decoded packets, then decodes all devices that transmit with $B-1$ energy units, and so on. We assume that a packet of energy j can be decoded if all higher-energy packets have been correctly decoded and removed. In this case, the battery profile of the interfering devices becomes $\hat{\boldsymbol{L}}^{(j)}=[\hat{L}_0^{(j)}\dots\hat{L}_B^{(j)}]$, where if $j>b$,

$$\hat{L}_i^{(j)} = \begin{cases} 0, & \text{if } i>j,\\ \bar{L}_i-1, & \text{if } i=j,\\ \bar{L}_i+1, & \text{if } i=b,\\ \bar{L}_i, & \text{if } i<j, i\le b,\end{cases} \tag{12}$$

and if $j=b$, then $\hat{L}_i^{(j)}=\bar{L}_i\mathbb{1}\{i\le b\}$ where $\mathbb{1}\{\cdot\}$ is the indicator function. It follows that the successful delivery probability is computed as

$$w_{b,\boldsymbol{L}} = \mathbb{E}_{\{\bar{L}_i\}_{i=1}^{B}}\bigg[\big(1-\epsilon_{b,\hat{\boldsymbol{L}}^{(b)}}\big)\prod_{j>b}\big(1-\epsilon_{j,\hat{\boldsymbol{L}}^{(b)}}\big)^{\bar{L}_j}\bigg], \tag{13}$$

where $\bar{L}_i$ follows the binomial distribution with parameters $(L_i,\alpha\pi_i)$. Note that $\hat{\boldsymbol{L}}^{(b)}$ is a function of $(b,\{\bar{L}_i\}_{i=1}^{B})$.

IV. AoI Analysis

We now derive the average AoI of a generic device.

1) Preliminaries: We denote by $B^{(s)}$ the battery level of the device of interest at the end of slot s. We let $X^{(s)}$ take value 1 if the device successfully delivers an update in the slot, and 0 otherwise. Furthermore, we denote the battery profile of the remaining $U-1$ devices at the end of slot s by $\boldsymbol{L}^{(s)}=[L_0^{(s)}\dots L_B^{(s)}]$. Consider an ancillary Markov chain $Z^{(s)}=(X^{(s)},B^{(s)},\boldsymbol{L}^{(s)})$. We next derive the transition probability from state $(x',b',\boldsymbol{\ell}')$ to state $(x,b,\boldsymbol{\ell})$. If $X^{(s-1)}=1$, the device of interest depletes its battery and thus cannot transmit an update in slot s. Therefore,

$$\begin{aligned}\mathbb{P}\big[(1,0,\boldsymbol{\ell}')\to(x,b,\boldsymbol{\ell})\big] &= \mathbb{1}\{x=0\}\\ &\cdot((1-\eta)\mathbb{1}\{b=0\}+\eta\mathbb{1}\{b=1\})\mathbb{P}\big[\boldsymbol{\ell}'\to\boldsymbol{\ell}\big],\end{aligned} \tag{14}$$

where $\mathbb{P}\big[\boldsymbol{\ell}'\to\boldsymbol{\ell}\big]$ is given in (8). If $X^{(s-1)}=0$, we separate the cases $X^{(s)}=1$ and $X^{(s)}=0$. First, $X^{(s)}=1$ if in slot s, the device generates and transmits a new update (w.p. $\alpha\pi_{b'}$), and the update is successfully decoded (w.p. $w_{b',\boldsymbol{\ell}'}$). In this case, the device depletes its battery after slot s. Therefore,

$$\mathbb{P}\big[(0,b',\boldsymbol{\ell}')\to(1,0,\boldsymbol{\ell})\big] = \alpha\pi_{b'}w_{b',\boldsymbol{\ell}'}\mathbb{P}\big[\boldsymbol{\ell}'\to\boldsymbol{\ell}\big]. \tag{15}$$

Second, $X^{(s)}=0$ if in slot s, the device either does not transmit or transmits but fails to deliver the packet. It follows that

$$\begin{aligned}&\mathbb{P}\big[(0,b',\boldsymbol{\ell}')\to(0,b,\boldsymbol{\ell})\big]\\ &=\big[(1-\alpha\pi_{b'}\mathbb{1}\{b'>0\})\big((1-\eta)\mathbb{1}\{b'=b<B\}\\ &\quad+\eta\mathbb{1}\{b=b'+1\}+\mathbb{1}\{b=b'=B\}\big)\\ &\quad+\alpha\pi_{b'}(1-w_{b',\boldsymbol{\ell}'})\mathbb{1}\{b=0\}\big]\mathbb{P}\big[\boldsymbol{\ell}'\to\boldsymbol{\ell}\big].\end{aligned} \tag{16}$$

2) Average AoI: As shown in Fig. 1, we denote by Y the *inter-refresh* time, i.e., the number of slots that elapse between two successive status updates for the device of interest. Right after a refresh, the current AoI is set to 1. By proceeding as in [3, Sec. III], we observe that the average AoI can be expressed in terms of the moments of Y as

$$\bar{\Delta} = 1+\frac{\mathbb{E}\big[Y^2\big]}{2\mathbb{E}[Y]}. \tag{17}$$

We next derive the moments of Y. Without loss of generality, we assign index 1 to the first slot contributing to the current inter-refresh time. We expand $\mathbb{E}[Y]$ as

$$\begin{aligned}\mathbb{E}[Y] = \sum_{x\in\{0,1\}}\sum_{b\in[0:B]}\sum_{\boldsymbol{\ell}\in\mathcal{L}}&\mathbb{E}\Big[Y|Z^{(1)}=(x,b,\boldsymbol{\ell})\Big]\\ &\cdot\mathbb{P}\big[Z^{(1)}=(x,b,\boldsymbol{\ell})\big].\end{aligned} \tag{18}$$

To compute $\mathbb{P}\left[Z^{(1)} = (x, b, \boldsymbol{\ell})\right]$, we note that the state in a slot with AoI refresh is of the form $(1, 0, \boldsymbol{\ell})$, and in slot 1, the state can only be $(0, 0, \boldsymbol{\ell})$ or $(0, 1, \boldsymbol{\ell})$. Therefore,

$$\mathbb{P}\left[Z^{(1)} = (x, b, \boldsymbol{\ell})\right] = \mathbb{1}\{x = 0, b \in \{0,1\}\} \cdot \frac{\sum_{\boldsymbol{\ell}' \in \mathcal{L}} p_Z((1, 0, \boldsymbol{\ell}'), (0, b, \boldsymbol{\ell}))}{\sum_{b \in \{0,1\}, \boldsymbol{\ell} \in \mathcal{L}} \sum_{\boldsymbol{\ell}' \in \mathcal{L}} p_Z((1, 0, \boldsymbol{\ell}'), (0, b, \boldsymbol{\ell}))}. \tag{19}$$

The conditional expectation $\mathbb{E}\left[Y | Z^{(1)} = (x, b, \boldsymbol{\ell})\right]$ can be derived via a first-step analysis [12, Sec. III-4]. If the packet from the device of interest is decoded in slot 1, i.e., $X^{(s)} = 1$, the inter-refresh time is 1. It follows that

$$\mathbb{E}\left[Y | Z^{(1)} = (1, b, \boldsymbol{\ell})\right] = 1, \quad b \in [0 : B], \boldsymbol{\ell} \in \mathcal{L}. \tag{20}$$

If $Z^{(1)} = (0, b, \boldsymbol{\ell})$, the inter-refresh time can be computed as the sum of the number of slots until a transmitted packet is successfully decoded. This can be conveniently computed by conditioning on the outcome of the first transition. Specifically, we define $r(b, \boldsymbol{\ell}) = \sum_{b'' \in [0:B], \boldsymbol{\ell}'' \in \mathcal{L}} \mathbb{P}\left[(0, b, \boldsymbol{\ell}) \to (1, b'', \boldsymbol{\ell}'')\right]$, $q((b, \boldsymbol{\ell}) \to (b'', \boldsymbol{\ell}'')) = \mathbb{P}\left[(0, b, \boldsymbol{\ell}) \to (0, b'', \boldsymbol{\ell}'')\right]$, and proceed as

$$\begin{aligned}\mathbb{E}\left[Y | Z^{(1)} = (0, b, \boldsymbol{\ell})\right] &= \\ & 1 + \sum_{z \in \{0,1\} \times [0:B] \times \mathcal{L}} \mathbb{E}\left[Y | Z^{(1)} = z\right] \mathbb{P}[(0, b, \boldsymbol{\ell}) \to z] \qquad (21) \\ &= 1 + r(b, \boldsymbol{\ell}) \\ &\quad + \sum_{b'' \in [0:B], \boldsymbol{\ell}'' \in \mathcal{L}} \mathbb{E}\left[Y | Z^{(1)} = (0, b'', \boldsymbol{\ell}'')\right] \\ &\quad \cdot q((b, \boldsymbol{\ell}) \to (b'', \boldsymbol{\ell}'')). \qquad (22)\end{aligned}$$

In (21), the Markov property ensures that the average duration, once the transition to state z has occurred, is equal to the one that we would have by starting from such state. Let $\boldsymbol{e}$ and $\boldsymbol{r}$ be vectors that contain $\mathbb{E}\left[Y | Z^{(1)} = (0, b, \boldsymbol{\ell})\right]$ and $r(b, \boldsymbol{\ell})$, respectively, sorted in the same order of possible values of $(b, \boldsymbol{\ell})$. Let $\mathbf{Q}$ be a matrix that contains $q((b, \boldsymbol{\ell}) \to (b'', \boldsymbol{\ell}''))$ where $(b, \boldsymbol{\ell})$ and $(b'', \boldsymbol{\ell}'')$ are sorted in such order. The full-rank system of equations obtained from (22) can be expressed compactly as $(\mathbf{I} - \mathbf{Q})\boldsymbol{e} = \mathbf{1} + \boldsymbol{r}$. Therefore, the conditional expectations $\mathbb{E}\left[Y | Z^{(1)} = (0, b, \boldsymbol{\ell})\right]$ are obtained as

$$\boldsymbol{e} = (\mathbf{I} - \mathbf{Q})^{-1} \boldsymbol{r}. \tag{23}$$

Substituting (19), (20), and (23) into (18), we obtain $\mathbb{E}[Y]$.

The second-order moment $\mathbb{E}\left[Y^2\right]$ is also computed via a first-step analysis. This yields

$$\mathbb{E}\left[Y^2 | Z^{(1)} = (1, b, \boldsymbol{\ell})\right] = 1, \quad b \in [0 : B], \boldsymbol{\ell} \in \mathcal{L}, \tag{24}$$

and

$$\begin{aligned}\mathbb{E}\left[Y^2 | Z^{(1)} = (0, b, \boldsymbol{\ell})\right] \\ &= 1 + 2 \sum_{z \in \{0,1\} \times [0:B] \times \mathcal{L}} \mathbb{E}\left[Y | Z^{(1)} = z\right] \mathbb{P}[(0, b, \boldsymbol{\ell}) \to z] \\ &\quad + \sum_{z \in \{0,1\} \times [0:B] \times \mathcal{L}} \mathbb{E}\left[Y^2 | Z^{(1)} = z\right] \mathbb{P}[(0, b, \boldsymbol{\ell}) \to z] \qquad (25) \\ &= -1 + 2\mathbb{E}\left[Y | Z^{(1)} = (0, b, \boldsymbol{\ell})\right] + r(b, \boldsymbol{\ell}) \\ &\quad + \sum_{b'' \in [0:B], \boldsymbol{\ell}'' \in \mathcal{L}} \mathbb{E}\left[Y^2 | Z^{(1)} = (0, b'', \boldsymbol{\ell}'')\right] \\ &\quad \cdot q((b, \boldsymbol{\ell}) \to (b'', \boldsymbol{\ell}'')). \qquad (26)\end{aligned}$$

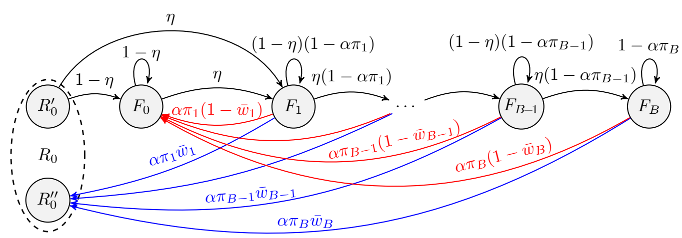

Fig. 3: Markov chain $\mathcal{M}_2$ to track the AoI refresh of a device.

Let $\boldsymbol{e}_2$ be a vector that contains $\mathbb{E}\left[Y^2 | Z^{(1)} = (0, b, \boldsymbol{\ell})\right]$ in the same order of $(b, \boldsymbol{\ell})$ as in $\boldsymbol{r}$ and $\boldsymbol{e}$. We express (26) compactly as $(\mathbf{I} - \mathbf{Q})\boldsymbol{e}_2 = -\mathbf{1} + 2\boldsymbol{e} + \boldsymbol{r}$, where $\boldsymbol{e}$ has been found in (23). It follows that the conditional expectations $\mathbb{E}\left[Y^2 | Z^{(1)} = (0, b, \boldsymbol{\ell})\right]$ are obtained as

$$\boldsymbol{e}_2 = (\mathbf{I} - \mathbf{Q})^{-1}(-\mathbf{1} + 2\boldsymbol{e} + \boldsymbol{r}). \tag{27}$$

Using (19), (24), and (27), we compute $\mathbb{E}\left[Y^2\right]$ via an expansion analogous to (18). Finally, the average AoI $\bar{\Delta}$ is obtained by inserting the computed moments of Y into (17).

The above exact computation becomes cumbersome as U and B increase. Specifically, computing the transition probabilities between all $2(B+1)\binom{U+B-1}{B}$ states of the chain Z is prohibitive for large U and B. Furthermore, the exact analysis of the AVP remains challenging. This motivates us to propose an approximate analysis in the next section.

V. Approximate AoI Analysis

To simplify the analysis, we ignore the time dependency of the battery profile of the devices whose performance is not tracked. Specifically, we assume the following.

Assumption 1: Given a device of interest, the battery profile $\boldsymbol{L}$ of the remaining $U - 1$ devices is *independent* across slots.

This assumption does not hold but allows us to analyze the behavior of the system, and—as we shall see—results in tight approximations of the average AoI and AVP for all scenarios explored. Under Assumption 1, the successful delivery probability of a device that transmits with b energy units is given by the average of $w_{b,\boldsymbol{L}}$ over $\boldsymbol{L}$, which is $\bar{w}_b$ given in (1). Then, the distribution of the inter-refresh time Y can be derived in closed form, as presented next.

1) Distribution of the Inter-Refresh Time Y: To track the behavior of the device of interest, we consider the Markov chain $\mathcal{M}_2$ presented in Fig. 3, which is obtained from $\mathcal{M}_1$ in Fig. 2 as follows. We first split the battery state 0 into two states: AoI refresh (R_0) and no AoI refresh (F_0). The state $b \in [B]$ in $\mathcal{M}_1$ is called F_b in $\mathcal{M}_2$. The device visits this state if its AoI value is not refreshed and its battery level is b. Next, we further split state R_0 into two states: R_0' (with only outgoing transitions from R_0) and R_0'' (with only incoming transitions to R_0). After some manipulations, we obtain the transition probabilities between these states under Assumption 1 as depicted in Fig. 3. The chain $\mathcal{M}_2$ is a *terminating Markov chain* with one absorbing state R_0'' and $B+1$ transient (i.e., non-absorbing) states $\{R_0', F_0, F_1, \dots, F_B\}$. Observe that the inter-refresh time Y is the absorption time into R_0'' when starting from R_0'. The distribution of the time until absorption of a terminating Markov chain is called the *discrete phase-type distribution* and has been analyzed in, e.g., [13, Sec. 2.2]. Leaning on this result, we characterize the distribution of Y in the following lemma, whose proof is omitted due to the space limitations.

Lemma 1 (Distribution of the inter-refresh time): Under Assumption 1, it holds that

$$\mathbb{P}[Y = y] = [\mathbf{T}^{y-1}\boldsymbol{t}_0]_1, \quad y = 1, 2, \dots, \tag{28}$$

$$\mathbb{P}[Y \le y] = 1 - [\mathbf{T}^{y}\mathbf{1}_{B+1}]_1, \quad y = 1, 2, \dots, \tag{29}$$

where $\boldsymbol{t}_0 = [0 \ \ \alpha\pi_1\bar{w}_1 \ \ \dots \ \ \alpha\pi_B\bar{w}_B]^{\mathsf{T}}$ and $\mathbf{T}$ is given in (30). Furthermore,

$$\mathbb{E}[Y] = [(\mathbf{I}_{B+1} - \mathbf{T})^{-1}\mathbf{1}_{B+1}]_1, \tag{31}$$

$$\mathbb{E}\left[Y^2\right] = \mathbb{E}[Y] + 2[(\mathbf{I}_{B+1} - \mathbf{T})^{-2}\mathbf{T}\mathbf{1}_{B+1}]_1, \tag{32}$$

$$\mathbb{E}\left[Y^{-1}\right] = [-\ln(\mathbf{I}_{B+1} - \mathbf{T})\mathbf{T}^{-1}\boldsymbol{t}_0]_1. \tag{33}$$

In (33), the logarithm of a matrix is defined as $\ln \mathbf{A} = \sum_{i=1}^{\infty}(-1)^{i+1}\frac{(\mathbf{A}-\mathbf{I}_m)^i}{i}$ for $\mathbf{A} \in \mathbb{R}^{m\times m}$.

2) Approximate Average AoI: By inserting the moments of Y given in (31) and (32) into (17), we obtain the average AoI under Assumption 1 as

$$\bar{\Delta} = \frac{3}{2} + \frac{[(\mathbf{I}_{B+1} - \mathbf{T})^{-2}\mathbf{T}\mathbf{1}_{B+1}]_1}{[(\mathbf{I}_{B+1} - \mathbf{T})^{-1}\mathbf{1}_{B+1}]_1}. \tag{34}$$

3) Approximate AVP: In an inter-refresh period of length Y slots, the AoI exceeds θ in the last $(Y - \theta + 1)^+$ slots (see Fig. 1). Therefore, for an observation time chosen uniformly at random from the period, the probability that the AoI exceeds θ is $(1 - (\theta-1)/Y)^+$. By averaging over Y, we obtain the AVP under Assumption 1 as

$$\zeta(\theta) = \mathbb{E}\left[(1 - (\theta - 1)/Y)^+\right] \tag{35}$$

$$= \mathbb{P}[Y \ge \theta] - (\theta - 1)\sum_{y=\theta}^{\infty}\frac{\mathbb{P}[Y = y]}{y} \tag{36}$$

$$= 1 - \mathbb{P}[Y \le \theta-1] - (\theta-1)\left(\mathbb{E}\left[Y^{-1}\right] - \sum_{y=1}^{\theta-1}\frac{\mathbb{P}[Y = y]}{y}\right) \tag{37}$$

$$= [\mathbf{T}^{\theta-1}\mathbf{1}_{B+1}]_1 + (\theta-1)\left([\ln(\mathbf{I}-\mathbf{T})\mathbf{T}^{-1}\boldsymbol{t}_0]_1 + \sum_{y=1}^{\theta-1} y^{-1}[\mathbf{T}^{y-1}\boldsymbol{t}_0]_1\right), \tag{38}$$

where (38) follows by inserting $\mathbb{P}[Y \le \theta-1]$, $\mathbb{E}\left[Y^{-1}\right]$, and $\mathbb{P}[Y = y]$, defined in (29), (33), and (28), respectively, into (37).

VI. Numerical Results

Throughout this section, we consider a slot length n of 100 channel uses and transmission rate R of 0.8 bits/channel use.

We first verify the accuracy of the exact and approximate analytical AoI analysis by a comparison with simulation results obtained from an implementation of the complete protocol operations of 10^5 slots. To enable the computation of the exact average AoI, we consider a small system with $U = 30$ and $B = 2$. We further set $\eta = 0.05$, $\theta = 600$, and $\sigma^2 = -20$ dB. In Fig. 4, we plot the average AoI (normalized by U) and AVP for the considered setting with capture. We consider two cases of transmission probabilities $\boldsymbol{\pi}$, namely, $\boldsymbol{\pi} = [1 \ 1]$ and $\boldsymbol{\pi} = [0 \ 1]$. In both cases, the approximate average AoI (34) matches well both the simulation result and exact analytical result. The approximate AVP (38) is also in agreement with the simulation result. This confirms that our approximate analysis provides accurate prediction of the AoI performance.

In the following, we report the approximate average AoI and AVP for a larger system with $U = 1000$, $B = 8$, $\eta = 0.005$, and $\theta = 8000$. We optimize the transmission probability $\boldsymbol{\pi}$ to obtain $\boldsymbol{\pi}^*_{\bar{\Delta}} = \arg\min_{\boldsymbol{\pi}\in[0,1]^B} \bar{\Delta}$, $\boldsymbol{\pi}^*_{\zeta} = \arg\min_{\boldsymbol{\pi}\in[0,1]^B} \zeta(\theta)$, $\boldsymbol{\pi}^*_{S} = \arg\max_{\boldsymbol{\pi}\in[0,1]^B} S$. We numerically solve these optimization problems using the Nelder-Mead simplex algorithm [14]. In Fig. 5, we plot the minimized average AoI, minimized AVP, and maximized throughput as functions of $U\alpha$, and compare with two baseline strategies: i) $\boldsymbol{\pi} = [\mathbf{0}^{\mathsf{T}}_{B-1} \ 1]$, i.e., a device only transmits with full battery, and ii) $\boldsymbol{\pi} = \mathbf{1}^{T}_{B}$, i.e., a device transmits a new update whenever possible. We see that the optimized $\boldsymbol{\pi}$ leads to significant improvement in all three metrics. The strategy $\boldsymbol{\pi} = \mathbf{1}^{\mathsf{T}}_{B}$ is close to optimal when $U\alpha$ is small, especially with capture. However, this strategy becomes highly suboptimal when $U\alpha$ increases since it causes many collisions. In contrast, the strategy with $\boldsymbol{\pi} = [\mathbf{0}^{\mathsf{T}}_{B-1} \ 1]$ has a decreasing gap to the optimal performance without capture when $U\alpha$ is large. (With $\boldsymbol{\pi} = [\mathbf{0}^{\mathsf{T}}_{B-1} \ 1]$, the performance with capture coincides with that without capture.) With capture, the minimized average AoI and maximized throughput are improved by about 10%

$$\mathbf{T} = \begin{bmatrix} 1-\eta & \eta & 0 & 0 & \dots & 0 & 0 \\ \alpha\pi_1(1-\bar{w}_1) & (1-\eta)(1-\alpha\pi_1) & \eta(1-\alpha\pi_1) & 0 & \dots & 0 & 0 \\ \alpha\pi_2(1-\bar{w}_2) & 0 & (1-\eta)(1-\alpha\pi_2) & \eta(1-\alpha\pi_2) & \dots & 0 & 0 \\ \vdots & \vdots & \vdots & \ddots & \ddots & \vdots & \vdots \\ \alpha\pi_{B-1}(1-\bar{w}_{B-1}) & 0 & 0 & 0 & \dots & (1-\eta)(1-\alpha\pi_{B-1}) & \eta(1-\alpha\pi_{B-1}) \\ \alpha\pi_B(1-\bar{w}_B) & 0 & 0 & 0 & \dots & 0 & 1-\alpha\pi_B \end{bmatrix} \tag{30}$$

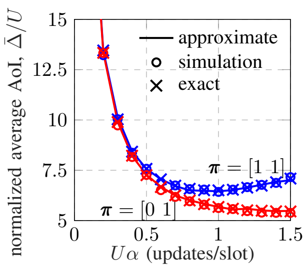

(a) Average AoI

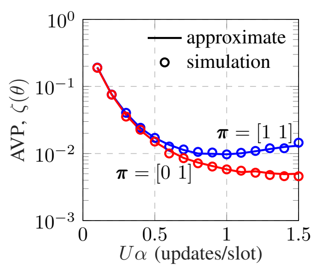

(b) AVP

Fig. 4: Average AoI and AVP vs. average total number of new updates in a slot ($U\alpha$). Here, $U = 30$, $\eta = 0.05$, $B = 2$, $n = 100$, $R = 0.8$, $\theta = 600$, $\sigma^2 = -20$ dB, and the decoder is with capture.

and 18.7%, respectively, for $U\alpha = 2.5$, compared to decoding without capture.

The optimized $\boldsymbol{\pi}$ can be different between metrics, although the $\boldsymbol{\pi}$ optimized for a metric also performs well for the other metrics, as illustrated by the performance of $\boldsymbol{\pi}_S^*$ in terms of the average AoI (Fig. 5(a)) and AVP (Fig. 5(b)). Without capture, the optimized $\boldsymbol{\pi}$ indicates that a device with higher battery level should transmit more likely. With capture, the devices should transmit with either low or high power, facilitating the decoding of high-energy packets and then low-energy packets after SIC. For example, for $U\alpha = 2.1$, $\boldsymbol{\pi}_{\bar{\Delta}}^*$ is $[0\ 0\ 0\ 0.68\ 1\ 1\ 1\ 1]$ without capture and $[0\ 0\ 1\ 1\ 0\ 0\ 0\ 1]$ with capture.

VII. Conclusions

We studied the impact of energy harvesting on information freshness in slotted ALOHA networks. Leaning on a Markovian analysis, we provided an exact analytical analysis of the average AoI, as well as an approximate analysis that results in easy-to-compute and accurate approximations of both the average AoI and AVP. Our main findings are as follows: i) transmitting a new update whenever possible is beneficial only for low update generation rates, while waiting for sufficient energy before transmitting is preferable for high update generation rates, ii) significant gains with respect to these baseline strategies can be achieved with an optimized strategy, iii) optimizing the strategy for one of the three metrics, namely, the average AoI, AVP, and throughput, comes at a small loss in the other metrics, iv) decoding with capture significantly outperforms decoding without capture, especially for high update generation rates.

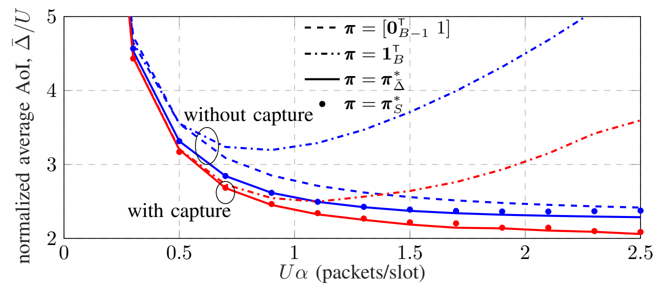

(a) Average AoI

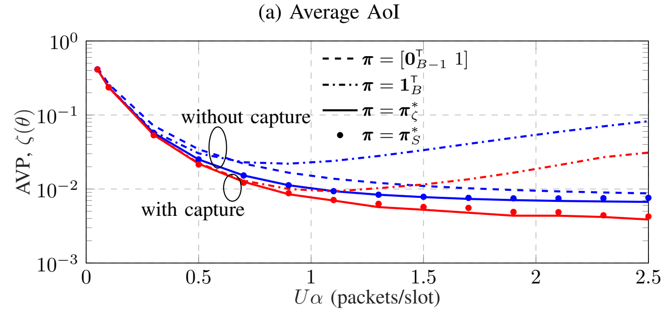

(b) AVP

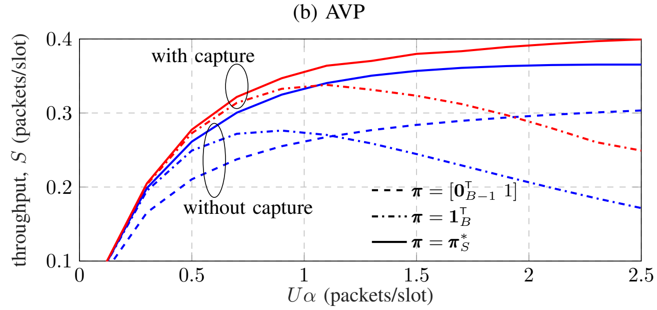

(c) Throughput

Fig. 5: Average AoI, AVP, and throughput vs. the total number of new updates in a slot ($U\alpha$) for different values of the transmission probabilities $\boldsymbol{\pi}$. Here, $U = 1000$, $\eta = 0.005$, $B = 8$, $n = 100$, $R = 0.8$, $\theta = 8000$, and $\sigma^2 = -20$ dB.

References

[1] A. Kosta, N. Pappas, and V. Angelakis, "Age of information: A new concept, metric, and tool," *Foundations and Trends in Networking*, vol. 12, no. 3, pp. 162–259, Nov. 2017.

[2] R. D. Yates and S. K. Kaul, "Status updates over unreliable multiaccess channels," in *Proc. IEEE Int. Symp. Inf. Theory (ISIT)*, Aachen, Germany, Jun. 2017, pp. 331–335.

[3] A. Munari, "On the value of retransmissions for age of information in random access networks without feedback," in *Proc. IEEE Glob. Commun. Conf. (GLOBECOM)*, Rio de Janeiro, Brazil, Dec. 2022, pp. 4964–4970.

[4] ——, "Modern random access: An age of information perspective on irregular repetition slotted ALOHA," *IEEE Trans. Commun.*, vol. 69, no. 6, pp. 3572–3585, Jun. 2021.

[5] A. Munari, F. Lazaro, G. Durisi, and G. Liva, "The dynamic behavior of frameless ALOHA: Stability, throughput, and age of information," *arXiv preprint arXiv:2301.10078*, 2023.

[6] P. Kamalinejad, C. Mahapatra, Z. Sheng, S. Mirabbasi, V. C. Leung, and Y. L. Guan, "Wireless energy harvesting for the Internet of Things," *IEEE Commun. Mag*, vol. 53, no. 6, pp. 102–108, Jun. 2015.

[7] A. M. Ibrahim, O. Ercetin, and T. ElBatt, "Stability analysis of slotted Aloha with opportunistic RF energy harvesting," *IEEE J. Sel. Areas Commun.*, vol. 34, no. 5, pp. 1477–1490, May 2016.

[8] H.-H. Choi, W. Shin, M. Levorato, and H. V. Poor, "Harvest-or-access: Slotted ALOHA for wireless powered communication networks," *IEEE Trans. Veh. Technol.*, vol. 68, no. 11, pp. 11 394–11 398, Nov. 2019.

[9] U. Demirhan and T. M. Duman, "Irregular repetition slotted ALOHA with energy harvesting nodes," *IEEE Trans. Wireless Commun.*, vol. 18, no. 9, pp. 4505–4517, Sep. 2019.

[10] Y. Polyanskiy, H. V. Poor, and S. Verdu, "Channel coding rate in the finite blocklength regime," *IEEE Trans. Inf. Theory*, vol. 56, no. 5, pp. 2307–2359, May 2010.

[11] J. Scarlett, V. Y. F. Tan, and G. Durisi, "The dispersion of nearest-neighbor decoding for additive non-Gaussian channels," *IEEE Trans. Inf. Theory*, vol. 63, no. 1, pp. 81–92, Jan. 2017.

[12] H. M. Taylor and S. Karlin, *An Introduction To Stochastic Modeling*, 3rd ed. London, UK: Academic Press, 1998.

[13] M. F. Neuts, *Matrix-Geometric Solutions in Stochastic Models: An Algorithmic Approach*. Baltimore, Maryland, USA: The Johns Hopkins University Press, 1981.

[14] J. A. Nelder and R. Mead, "A simplex method for function minimization," *The computer journal*, vol. 7, no. 4, pp. 308–313, Jan. 1965.